

to understand sQGP through non-topological FL model

Song Shu

Faculty of Physics and Electronic Technology, Hubei University, Wuhan 430062, China

Jia-Rong Li

Institute of Particle Physics, Hua-Zhong Normal University, Wuhan 430079, China

The non-topological FL model is studied at finite temperature and density. The soliton solutions of the FL model in deconfinement phase transition are solved and thoroughly discussed for different boundary conditions. We indicate that the solitons before and after the deconfinement have different physical meanings: the soliton before deconfinement represents hadron, while the soliton after the deconfinement represents the bound state of quarks which leads to a sQGP phase. The corresponding phase diagram is given.

PACS numbers: 25.75.Nq, 12.39.Ki, 11.10.Wx

I. INTRODUCTION

An important discovery at Relativistic Heavy Ion Collider (RHIC) in recent years is the realization of strongly interacting Quark Gluon Plasma (sQGP) [1–3]. For the collective effects from RHIC experiments, known as radial and elliptic flow, the QGP could be well described by ideal hydrodynamics. It implies that the QGP at RHIC is the most perfect fluid [4–6]. For this reason, Shuryak has pointed out there should be lots of bound states [1] especially for light and heavy qq bound states at $T_c < T < 4T_c$, where T_c is the transition temperature. For the physical quark mass the QCD transition is a non-singular crossover at finite temperature. In recent lattice results, at high temperatures and small densities, it is a crossover from hadronic phase to QGP phase [7, 8]. From recent theoretical studies, we have realized the rich phases of QCD theory, such as color superconducting phase [9], pion condensation [10], color glass condensate and quarkyonic phase [11]. Now the RHIC results tell us that after deconfinement, the quarks are not free immediately, as we usually thought for a weakly coupled QGP (wQGP), but still in strong coupled state which leads to a new state of nuclear matter as the sQGP. How to understand the formation mechanism of sQGP is an important problem [12]. As we know, there are confine potential and color coulomb potential between quarks in vacuum, know as $V \sim \alpha/r + kr$. With temperature T increased to some critical temperature, the confine potential disappears, while the coulomb potential remains, which could still be very strong [13]. Thus in literatures, the effective coulomb potential has been often used to describe the strong interaction of sQGP [14]. But from the theoretical point of view, it is lack of a more fundamental theoretical model to understand these bound states of quarks. In this paper we wish to use non-topological FL model to study this problem.

FL model has been widely discussed in past decays [15–17]. It has been very successful in describing phenomenologically the static properties of hadrons and their behaviors at low energy. The model consists of quark fields interacting with a phenomenological scalar field σ . The σ field is introduced to describe the complicated nonperturbative features of QCD vacuum. It naturally gives a color confinement mechanism in QCD theory. The model has been also extended to finite temperatures and densities to study deconfinement phase transition [18–21]. However it seems that the deep meaning of the soliton solutions in deconfinement phase transition has not been revealed in the past studies. The main purpose of this paper is to study in detail the properties of the solitons in FL model before and after deconfinement, and provide a natural explanation and description of sQGP through this effective theoretical model.

The organization of this paper is as follows: in section 2 we give a brief introduction of FL model. The field equations and the effective potential are derived. In section 3, the soliton equation of FL model is solved for different boundary conditions and the physical meanings of these solitons in deconfinement are thoroughly discussed. In section 4, a phase diagram of deconfinement phase transition is given. The last section is the summary.

II. FL MODEL AND THE EQUATIONS

We start from the Lagrangian of the FL model,

$$\mathcal{L} = \bar{\psi}(i\gamma_\mu\partial^\mu - g\sigma)\psi + \frac{1}{2}(\partial_\mu\sigma)(\partial^\mu\sigma) - U(\sigma), \quad (1)$$

where

$$U(\sigma) = \frac{1}{2!}a\sigma^2 + \frac{1}{3!}b\sigma^3 + \frac{1}{4!}c\sigma^4 + B. \quad (2)$$

ψ represents the quark field, and σ denotes the phenomenological scalar field. a, b, c, g and B are the constants which are generally fitted in with producing the properties of hadrons appropriately.

For the thermal equilibrium system, the σ field will be replaced by $\bar{\sigma} + \sigma'$, where $\bar{\sigma}$ is the Gibbs thermal average of the σ field, and σ' is the fluctuation. At mean field approximation, one can obtain the field equations as follows,

$$(i\gamma_\mu\partial^\mu - g\bar{\sigma})\psi = 0, \quad (3)$$

$$\partial_\mu\partial^\mu\bar{\sigma} = -\frac{\partial V_{eff}}{\partial\bar{\sigma}}, \quad (4)$$

where V_{eff} is one loop effective potential at finite temperature and density. Notice that at mean field approximation the quantum corrections have been neglected. The V_{eff} could be derived through finite temperature field theory [20, 21],

$$V_{eff} = U(\bar{\sigma}) + \frac{1}{\beta} \int \frac{d^3\mathbf{p}}{(2\pi)^3} \ln(1 - e^{-\beta E_\sigma}) - \frac{\gamma}{\beta} \int \frac{d^3\mathbf{p}}{(2\pi)^3} \left[\ln(1 + e^{-\beta(E_q - \mu)}) + \ln(1 + e^{-\beta(E_q + \mu)}) \right], \quad (5)$$

in which β is the inverse temperature, μ is the chemical potential, and γ is a degenerate factor, $\gamma = 2(\text{spin}) \times 2(\text{flavor}) \times 3(\text{color})$. Besides $E_\sigma = \sqrt{\vec{p}^2 + m_\sigma^2}$, $E_q = \sqrt{\vec{p}^2 + m_q^2}$, where $m_q = g\bar{\sigma}$ and $m_\sigma^2 = a + b\bar{\sigma} + \frac{1}{2}c\bar{\sigma}^2$ are the effective masses of the quark and σ field respectively.

From equation (4), one could see that the properties of the soliton field $\bar{\sigma}$ depend completely on the effective potential V_{eff} . As known, by the effective potential at finite temperature and density, one can study the deconfinement phase transition in FL model. Thus the properties of solitons in deconfinement, especially the relations between solitons and deconfinement, could be well studied through solving the equation (4) at finite temperature and density.

In our calculation, the parameters are chosen to be $a = 17.7\text{fm}^{-2}$, $b = -1457.4\text{fm}^{-1}$, $c = 20000$, $g = 12.16$. The effective mass of σ field is fixed at $m_\sigma = 550\text{MeV}$ [20]. At zero temperature and density, the V_{eff} is just the $U(\bar{\sigma})$ and could be plotted in Fig.1. There are two minima: one corresponds to the perturbative vacuum at $\bar{\sigma} = 0$, another corresponds to the physical vacuum at $\bar{\sigma} = \sigma_v$.

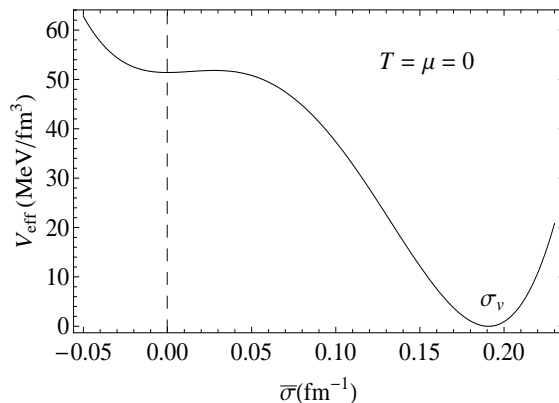


FIG. 1: The effective potential at zero temperature and density .

III. THE SOLITON SOLUTIONS AND SQGP IN DECONFINEMENT

For the static and spherically symmetric soliton field, the equation (4) becomes

$$\frac{d^2\bar{\sigma}}{dr^2} + \frac{2}{r} \frac{d\bar{\sigma}}{dr} = \frac{\partial V_{eff}}{\partial\bar{\sigma}}. \quad (6)$$

We will solve this equation numerically. A standard numerical package COLSYS will be used for the numerical calculation [22].

For solving the soliton equation (6), one should first determine the boundary condition. There are two different cases of the boundary conditions for solving the equation [17, 23]. In the following the two cases will be studied separately.

A. Boundary condition I

In this case, we may consider the mechanical analog in which there is a point particle at “position” σ and a time “ r ”, moving in a “potential” $-V_{eff}$. The discussions about this mechanical analog could be found in Ref. [23]. Equation (6) is then the movement equation of the particle. Because the energy conservation will be applied in this case, the second term at l.h.s of equation (6) will be omitted. Thus the equation becomes

$$\frac{d^2\bar{\sigma}}{dr^2} = \frac{\partial V_{eff}}{\partial \bar{\sigma}}. \quad (7)$$

In order to determine the boundary condition, suppose at “time” $r = -\infty$, the “position” of the particle is at $\bar{\sigma} = 0$. From Fig.1, if the particle is pushed very gently to start moving, the particle will move to another point just at $\bar{\sigma} = \sigma_a$ where $V_{eff}(0) = V_{eff}(\sigma_a)$, noticing that the particle is moving in the “potential” $-V_{eff}$. Because of energy conservation, the particle will then move back and return to the point $\bar{\sigma} = 0$. Thus one could obtain the following boundary condition,

$$\bar{\sigma}(r = -\infty) = 0, \quad \bar{\sigma}(r = +\infty) = 0. \quad (8)$$

From Fig.1, the physical vacuum $\bar{\sigma} = \sigma_v$ is stable, and $B = V_{eff}(0) - V_{eff}(\sigma_v)$ is the bag constant. The quarks are confined in a soliton bag. At zero temperature and density, the soliton solution represents a hadron.

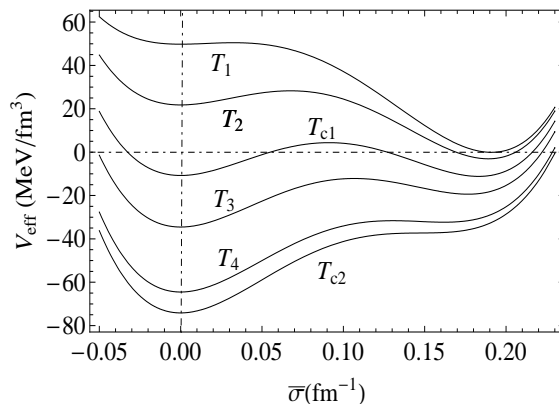


FIG. 2: The effective potential for different temperatures: $T_1 = 50MeV$, $T_2 = 100MeV$, $T_{c1} = 121MeV$, $T_3 = 130MeV$, $T_4 = 140MeV$ and $T_{c2} = 143MeV$.

At finite temperature, the V_{eff} could be plotted in Fig.2. There are two critical temperatures T_{c1} and T_{c2} . At T_{c1} , the two minima degenerate and the bag constant $B = 0$. At T_{c2} , the minimum $\bar{\sigma} = \sigma_v$ just vanishes. For different configurations of V_{eff} , the equation (7) could be numerical solved by the numerical package COLSYS. However the V_{eff} is highly non-linear in $\bar{\sigma}$ as shown in equation (5). It could not be directly used in COLSYS evaluation. At finite temperature, as the V_{eff} could be plotted as shown in Fig.2, we can fit the curve in terms of σ^2 , σ^3 and σ^4 with the effective parameters $a(T)$, $b(T)$ and $c(T)$. That means

$$V_{eff} = \frac{1}{2!}a(T)\sigma^2 + \frac{1}{3!}b(T)\sigma^3 + \frac{1}{4!}c(T)\sigma^4 + B(T). \quad (9)$$

In this form, the V_{eff} could be applied in COLSYS for the numerical calculation. In the following we will solve equation (7) and discuss the soliton solutions for different configurations of V_{eff} .

At $T < T_{c1}$, the physical vacuum at $\bar{\sigma} = \sigma_v$ is stable. The bag constant $B \neq 0$ and its value decreases with temperature increasing. The corresponding quarks are confined. The equation (7) could be numerically solved and the soliton solutions are plotted in Fig.3a. One could see that the solitons at temperature $T < T_{c1}$ do not change so much when compared to that at zero temperature except the peaks of the solitons become higher when temperature increases. The quarks keep confined in a hadronic state until the critical temperature $T = T_{c1}$ the two vacuums degenerate. At this time, still required by the energy conservation the boundary condition is

$$\bar{\sigma}(r = -\infty) = 0, \quad \bar{\sigma}(r = +\infty) = \sigma_v. \quad (10)$$

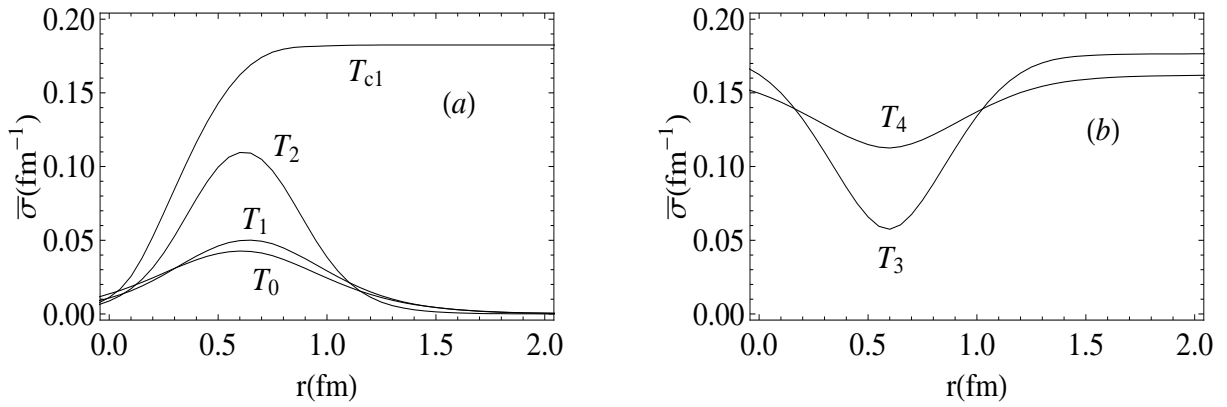


FIG. 3: The soliton solutions for boundary condition I at different temperatures. (a) $T_0 = 0MeV$, $T_1 = 50MeV$, $T_2 = 100MeV$ and $T_{c1} = 121MeV$. (b) $T_3 = 130MeV$ and $T_4 = 140MeV$.

The soliton becomes topological as shown in Fig.3a. As the bag constant $B = 0$ at this time, the hadrons are destructed and the quarks are deconfined.

If we keep increasing temperature to $T_{c1} < T < T_{c2}$, from Fig.2, the perturbative vacuum $\bar{\sigma} = 0$ is stable. The equation (7) will be solved under the boundary condition

$$\bar{\sigma}(r = -\infty) = \sigma_v, \quad \bar{\sigma}(r = +\infty) = \sigma_v. \quad (11)$$

The soliton solutions could be plotted in Fig.3b. The soliton solutions still exist but become very different from those at $T < T_{c1}$. The peaks of the solitons become downward. When temperature increasing, they become flat. These solitons do not represent hadrons any more but the bound states of quarks. Though the quarks are deconfined, they are still in strong coupled states. That is to say the system is in a sQGP phase. Until $T \geq T_{c2}$, the physical vacuum $\bar{\sigma} = \sigma_v$ vanishes and only the perturbative vacuum $\bar{\sigma} = 0$ exists, has the soliton solution disappeared. At this time the quarks become free. The system goes into a quasi-free gas phase of QGP.

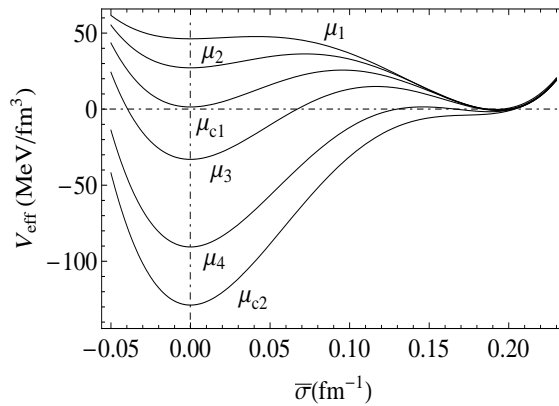


FIG. 4: The effective potential for different chemical potentials: $\mu_1 = 100MeV$, $\mu_2 = 200MeV$, $\mu_{c1} = 255MeV$, $\mu_3 = 300MeV$, $\mu_4 = 350MeV$ and $\mu_{c2} = 375MeV$.

At finite temperature and density, we could also make the similar discussions. In Fig.4, we show the V_{eff} at $T = 50MeV$ and different chemical potentials. There are also two critical chemicals μ_{c1} and μ_{c2} . At μ_{c1} the two vacuums degenerate; at μ_{c2} the vacuum of $\sigma \neq 0$ just vanishes. The corresponding soliton solutions are plotted in Fig.5a and Fig.5b. It is clear that at $\mu \leq \mu_{c1}$, the system is in a hadronic phase; at $\mu_{c1} < \mu < \mu_{c2}$, the system is in a sQGP phase; at $\mu \geq \mu_{c2}$, the system becomes quasi-free gas of QGP.

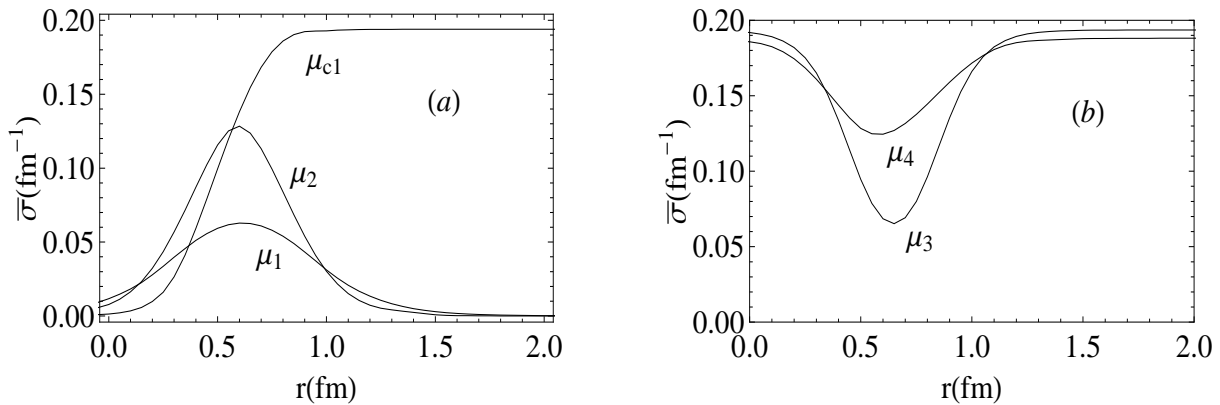


FIG. 5: The soliton solutions for boundary condition I at different chemical potentials. (a) $\mu_1 = 100MeV$, $\mu_2 = 200MeV$ and $\mu_{c1} = 255MeV$. (b) $\mu_3 = 300MeV$ and $\mu_4 = 350MeV$.

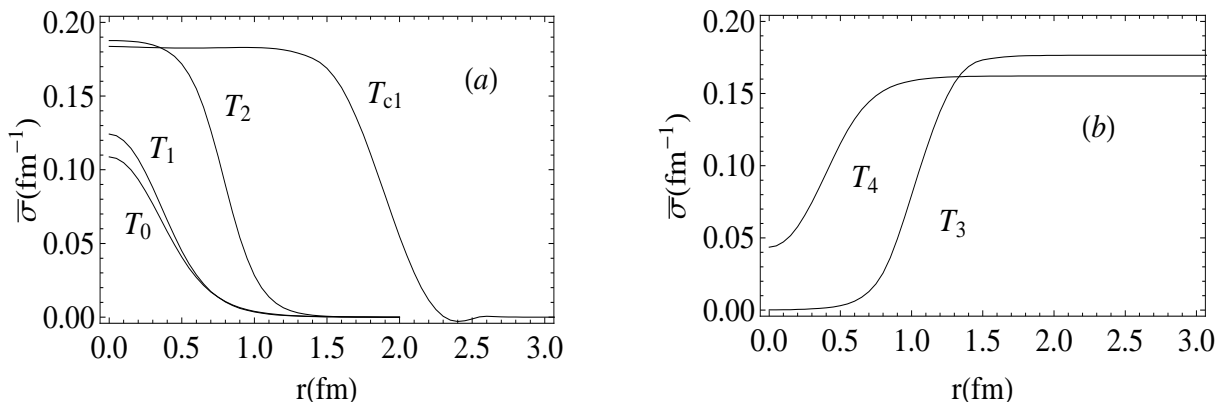


FIG. 6: The soliton solutions for boundary condition II at different temperatures. (a) $T_0 = 0MeV$, $T_1 = 50MeV$, $T_2 = 100MeV$ and $T_{c1} = 121MeV$. (b) $T_3 = 130MeV$ and $T_4 = 140MeV$.

B. Boundary condition II

In this case, at $T \leq T_{c1}$, the boundary condition is taken as

$$\left. \frac{d\bar{\sigma}}{dr} \right|_{r=0} = 0, \quad \bar{\sigma}|_{r \rightarrow \infty} = 0. \quad (12)$$

The equation (6) could be numerically solved at finite temperature and density for different configurations of V_{eff} .

From Fig.2, at $T < T_{c1}$, the soliton solutions are plotted in Fig.6a. The physical vacuum $\bar{\sigma} = \sigma_v$ is stable and The bag constant $B \neq 0$. The solitons still represent that the quarks are confined and the system is in a hadronic phase. Until $T = T_{c1}$ the system are deconfined. The corresponding soliton is also plotted in Fig.6a.

At $T_{c1} < T < T_{c2}$, the boundary condition is

$$\left. \frac{d\bar{\sigma}}{dr} \right|_{r=0} = 0, \quad \bar{\sigma}|_{r \rightarrow \infty} = \sigma_v. \quad (13)$$

The soliton solutions are solved and plotted in Fig.6b. These solitons are quite different from those at $T < T_{c1}$. As the system is already deconfined, these solitons represent the quarks are in a bound state. The system is in a sQGP phase. At $T > T_{c2}$, there are no soliton solution any more, the system goes to a quasi-free gas of QGP.

For different chemical potentials at fixed temperature $T = 50MeV$, according to the V_{eff} as shown in Fig.4, the corresponding soliton solutions could be solved and plotted in Fig.7a and Fig.7b. It is clear that at $\mu < \mu_{c1}$ it is a hadronic phase; at $\mu_{c1} < \mu < \mu_{c2}$, it is in a sQGP phase; at $\mu > \mu_{c2}$ it is a quasi-free gas of QGP.

From above discussions, it is clear that for the two different boundary conditions, the physical meaning of the solitons are the same: before deconfinement the solitons represent hadrons while after deconfinement the solitons

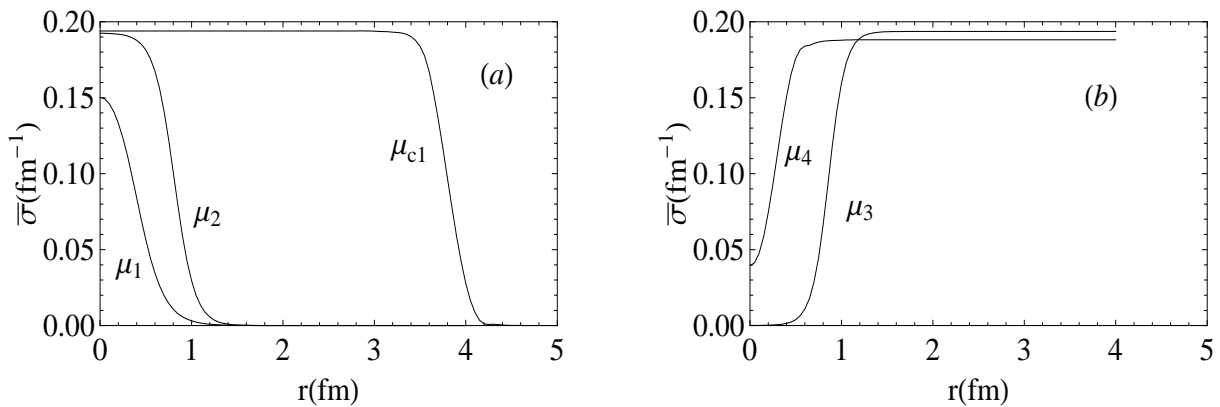


FIG. 7: The soliton solutions for the boundary condition II at different chemical potentials. (a) $\mu_1 = 100\text{MeV}$, $\mu_2 = 200\text{MeV}$ and $\mu_{c1} = 255\text{MeV}$. (b) $\mu_3 = 300\text{MeV}$ and $\mu_4 = 350\text{MeV}$.

represent bound states of quarks. For the two cases, the phase structure of deconfinement remains unchanged and unique.

IV. THE PHASE DIAGRAM

Now we are in a position to plot the phase diagram of deconfinement phase transition in FL model. When the chemical potential is fixed, one could obtain two critical temperatures. Increasing the chemical potential to another fixed value, the other two corresponding critical temperatures could be obtained, and so on. The $\mu - T$ phase diagram could be plotted as shown in Fig.8. The full line is the dividing line between hadronic phase and deconfined quark phase. The dashed line further divides the deconfined quark phase into the sQGP phase and the wQGP phase.

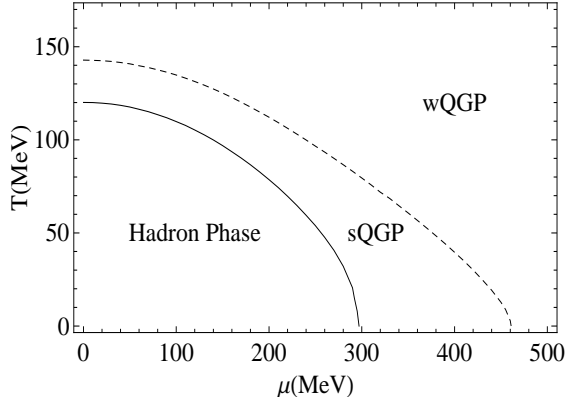


FIG. 8: The phase diagram of deconfinement in the FL soliton model.

V. SUMMARY

In this paper the soliton solutions in FL model at finite temperatures and densities have been thoroughly discussed for two kinds of different boundary conditions. The physical interpretations of the solitons in deconfinement phase transition have been given. As in FL model the system is deconfined at the time that the bag constant becomes zero, we indicate that the solitons before deconfinement are hadrons, while the solitons after deconfinement represent the strong coupled bound states of quarks, which leads to the sQGP phase. The QCD phase structure still needs lots of thorough investigations, especially for the finite density areas, where the results are often model dependent. Here we only present a possible phase diagram based on FL model. The phase structure of deconfinement phase transition

here is qualitatively consistent with that of Shuryak [1]. The whole phase diagram is divided into three phases: the hadronic phase, the sQGP phase and the wQGP phase.

Acknowledgments

We are thankful to Hong Mao for helpful discussions on numerical calculations. This work was supported in part by the National Natural Science Foundation of China with No. 10905018 and No. 10675052.

-
- [1] E.V. Shuryak and I. Zahed, Phys.Rev. C49 (2004) 021901.
 - [2] G.E. Brown, C-H. Lee, M. Rho and E.V. Shuryak, Nucl.Phys. A740 (2004) 171.
 - [3] M. Gyulassy and L. McLerran, Nucl. Phys. A750, (2005) 30.
 - [4] D. Teaney, J. Lauret and E.V. Shuryak, Phys. Rev. Lett. 86 (2001) 4783.
 - [5] P.F. Kolb, P. Huovinen, U. Heinz and H. Heiselberg, Phys. Lett. B500 (2001) 232.
 - [6] D. Teaney, Phys.Rev. C68 (2003) 034913.
 - [7] Z. Fodor and S.D. Katz, J. High Energy Phys. 050 (2004) 0404.
 - [8] F. Karsch, PoSCPOD07 (2007) 026; PoSLAT2007 (2007) 015.
 - [9] M. Alford, K. Rajagopal and F. Wilczek, Phys. Lett. B422 (1998) 247; K. Rajagopal, Prog. Theor. Phys. Suppl. 131 (1998) 619; R. Rapp, T. Schafer, E.V. Shuryak and M. Velkovsky, Phys. Rev. Lett. 81 (1998) 53.
 - [10] D.T. Son and M.A. Stephanov, Phys. Rev. Lett. 86 (2001) 592; K. Splittorff, D.T. Son, and M.A. Stephanov, Phys. Rev. D64 (2001) 016003; J.B. Kogut and D. Toublan, Phys. Rev. D64 (2001) 034007.
 - [11] L.D. McLerran and R. Venugopalan, Phys. Rev. D49 (1994) 2233; E. Iancu and L. McLerran, Phys. Lett. B510 (2001) 145; L. McLerran and R. Pisarski, Nucl. Phys. A796 (2007) 83.
 - [12] T.D. Lee, Nucl. Phys. A750 (2005) 1.
 - [13] K. Yagi, T. Hatsuda and Y. Miake, Quark-Gluon plasma, Cambridge Univ. Press (2005).
 - [14] D. Zwanziger, Phys. Rev. Lett. 90 (2003) 102001; Phys. Rev. D 70 (2004) 094034.
 - [15] R. Friedberg and T.D. Lee, Phys. Rev. D15, (1977) 1694; D16, (1977) 1096; D18, (1978) 2623.
 - [16] R. Goldflam and L. Wilets, Phys. Rev. D25 (1982) 1951.
 - [17] M.C. Birse, Prog. Part. Nucl. Phys. 25 (1990) 1.
 - [18] H. Reinhardt, B.V. Dang and H. Schulz, Phys. Lett. B159 (1985) 161.
 - [19] M. Li, M.C. Birse and L. Wilets, J.Phys. G13 (1987) 1.
 - [20] E.K. Wang, J.R. Li and L.S. Liu, Phys. Rev. D41 (1990) 2288; S. Gao, E.K. Wang and J.R. Li, Phys. Rev. D46 (1992) 3211; S.H. Deng and J.R. Li, Phys.Lett. B302 (1993) 279.
 - [21] H. Mao, R.K. Su and W.Q. Zhao, Phys. Rev. C74 (2006) 055204; H. Mao, M.J. Yao and W.Q. Zhao, Phys. Rev. C77 (2008) 065205.
 - [22] U. Ascher, J. Christiansen and R.D. Russell, ACM Trans. Math. Software 7 (1981) 209.
 - [23] T.D. Lee, Particle Physics and Introduction to Field Theory, Harwood Academic, New York (1981).